THE PRECISION PRODUCTION OF UNIFORM DROPLETS

By

EDWARD FENTON COOKE, III

Bachelor of Science

Rice University

Houston, Texas

1961

Submitted to the faculty of the Graduate School of
the Oklahoma State University
in partial fulfillment of the requirements
for the degree of
MASTER OF SCIENCE
August, 1962

THE PRECISION PRODUCTION OF UNIFORM DROPLETS

Thesis Approved:

Jerald D. Parker
Thesis Adviser

R. F. Lowery

Dean of the Graduate School

PREFACE

In any fundamental study of mists, it is necessary to understand the behavior of the individual droplets. The total effect of the whole mist is found by weighting the effect of each size range of droplet by its percentage of the total. To study the effect of each size droplet some method must be found of producing droplets of a given size and in such a manner as to place them available for ready observation.

It is the purpose of this study to provide some insight into the development of a totally predictable droplet generator and to establish a suitable method of observing droplet formation. As these difficulties were being met, new problems began to develop such as the type of flow in vibrating tubes, the method of separation of the droplet from the tube, and the mode shape of the vibrating tube. The experimentation was hampered by the fragility of the glass capillary tubing and by the length of time necessary to determine the droplet size. The latter of these problems was resolved late in the experimentation, but the former has not yet been solved.

Indebtedness is acknowledged to Dr. J. D. Parker for his valuable guidance and to the School of Mechanical Engineering of Oklahoma State University for its assistance in the building and procuring of equipment. Acknowledgment is also made to The Rice University for its aid in the building of the first mechanical prototype.

TABLE OF CONTENTS

LIST OF FIGURES

CHAPTER I

INTRODUCTION

Previous Experience

There are two basic fields in which the study of small droplets is needed: heat transfer to mists, and the study of injector nozzles as in diesel engines and aerosol bombs. This paper is connected with the former and is restricted to the investigation of water droplets, but the same principles, with the appropriate changes in surface tension and density, will also apply to other fields. This investigation was also limited to the production of droplets between 50 and 100 microns in diameter since these seem to be the sizes most useful in determining heat transfer to a mist of steam and water droplets in turbulent flow through a tube. (Parker, 1961).

The problem was and still remains that of reliably producing droplets within the given size range such that all the droplets fall in one area. This is necessary, for example, if one is to photograph the droplets as they react with a hot surface.

In one reference, Dimmock (1950) claims to have done exactly this using a vertical tube with a hypodermic needle attached. The tube was vibrated by a magnet at 50 cps. producing one small droplet at the end of each stroke. Reproduction of this experiment was tried using a slant point needle rather than the side ejection needle

used by Dimmock, and it was found that not only was the power requirement huge, but the tube would not vibrate in one plane. Instead, the end of the tube would describe an ellipse, and the drops would separate in a progression around the ellipse. Concurring with the results is Parker (1961) who tried the same experiment with a fine capillary of glass drawn from a larger tube. Another interesting point is that Dimmock used a side ejection hypodermic needle, similar to the type of needle used to inflate a football, which seems to be unobtainable in this country except through special production by a watchmaker. In Dimmock's article, a picture was shown of a 100 micron droplet separating from the needle which had a diameter comparable to that of the droplet. The needle must have been extremely small since a 100 micron droplet is about 0.004 inches in diameter. Needles this small are obtainable, but the author was unable to locate any with a hole in the side. Perhaps a needle might be manufactured from a precision metering orifice or from existing capillary tubing.

Parker's experiment was more enlightening in that he produced droplets in the 50 to 100 micron diameter size range by using a vertical glass capillary about 0.010 inches O. D. with one end fixed to a frame and the other end free. The tube was excited by a small piece of iron wire wrapped around it which in turn was under the influence of an electromagnet driven by an audio-oscillator. Parker found that the tube described an ellipse as it oscillated and that the droplets would separate in a progression around the ellipse. The static head on the tube could be varied, and the progression rate would change accordingly. He also noted that there was a relationship between the

head and the droplet size. The elliptic path was caused by the round tube having the same natural frequencies in all directions. The progression of the droplet separation around the ellipse was due to the fact that the head applied to the capillary was such that the droplet was fully formed either before or after the position of the previous droplet separation. The droplets must separate at the same point in the cycle each time or they will progress around the path followed by the tip of the reed. These facts were the basis for the experiments described in this thesis. It will be shown that there is a definite relationship between head, frequency, and amplitude of vibration which will be called "the phasing equation." When correctly phased, Parker's apparatus would provide a constant stream of small droplets in one trajectory.

This particular method is extremely sensitive to minute changes in viscosity, surface tension, and amplitude. When photographs were to be made, this sensitivity caused the droplets to begin to precess once more. The added heat from the flood lanps changed the viscosity and the system's phasing.

CHAPTER II

DROPLET MEASUREMENT

Introduction

In developing a droplet generator, a method of determining size and uniformity is required. Droplets of approximately 100 microns in diameter are very difficult to see with the naked eye; however, if a light is placed about 135° from the observer's eye, the droplets can be seen as a light misty trail resembling cigarette smoke. Exact measurement of these droplets poses several problems dealing with the realms of focus, distortion, or evaporation.

Another difficulty is encountered when trying to photograph the droplets. As has been mentioned previously, the droplets can only be seen by shining a light through them; however, the light has a tendency to blind the camera. Coupling this fact with the critical scaling factors and shutter timings necessary for the photographs to be true renders this method of measurement difficult. In spite of these involvements, the photography of mists is quite common as evidenced by the methods presented in spray literature. (DeJuhasz, 1959).

If the droplets are caught in oil, toluene, or any of the several other substances in which water is immiscible, then the droplets will remain on surface due to the surface tension of the catching liquid where they may be microscopically studied. The evaporation rate of a

100 micron diameter droplet is extremely high; therefore, before the microscope can be focused, the droplet may not only be less than its original size, but may not be there at all! If the droplets are ever to be measured, they must retain their original size for a suitable length of time.

Stoke's Law Method

This conclusion gave rise to a more subtle method of measuring the size of the droplets, i.e. an application of Stoke's law to a droplet falling in a viscous fluid. The problem here was to get the droplets past the surface tension barrier and into the fluid so that their falling rate could be determined.

The problem was solved in the following manner. The droplets were caught in a 10 ml graduate filled with 9 ml of S.A.E. 30 motor oil. One ml of the same oil was poured on top of the droplets leaving them sandwiched between the two layers of oil thereby free in the center of the oil where the fall rate could be determined.

The graduate selected for this experiment had the one ml graduation lines entirely around the circumference every 0.391 inches describing the time start and stop planes. Individual droplets could be seen by placing a light in the correct position behind the graduate. The single droplet's falling time between the start and stop planes was measured with a stop watch. Stoke's law predicts that the steady state velocity of a slowly moving sphere in a viscous liquid is:

$$V = \frac{\Delta x}{T} = \frac{2}{9} \frac{r^2 g}{\mu} (\rho - \rho_o) \quad , \quad N_{Re_D} < 1$$

or rearranging

$$d^2 = \frac{18\mu}{\rho g \left(1-\frac{\rho_o}{\rho}\right)} \frac{\Delta x}{} T^{-1}$$

where ρ = density of the sphere

ρ_o = density of the liquid

Δx = the distance traveled in time T seconds. (Streeter, 1958)

The oil was first calibrated by dropping lead bird shot into it and making a least squares fit with points where $0.668 < N_{Re_D} < .825$ to the form

$$d^2 = AT^{-1}$$

$$A = 171.154$$

Using the subscripts L and W to mean "lead sphere" and "water droplet" respectively, then this correction formula for the calibration of the oil is found:

$$d_W^2 = \frac{\rho_L}{\rho_W} \frac{\left(1-\frac{\rho_o}{\rho_L}\right)}{\left(1-\frac{\rho_o}{\rho_W}\right)} \frac{\Delta x_W}{\Delta x_L} d_L^2 T_L T_W^{-1}$$

$$\frac{\rho_L}{\rho_W} = 11.3$$

$\frac{\rho_o}{\rho_W}$ was found to be 0.895 by using a two-leg manometer as shown in Figure 1. It is interesting to note here that the water and the oil are nearly the same density, a fact that has a great deal of bearing on the distortion of the droplet when immersed in oil as will be discussed later in this chapter.

$$\frac{\rho_o}{\rho_L} = \frac{\rho_o}{\rho_W} \frac{\rho_W}{\rho_L}$$

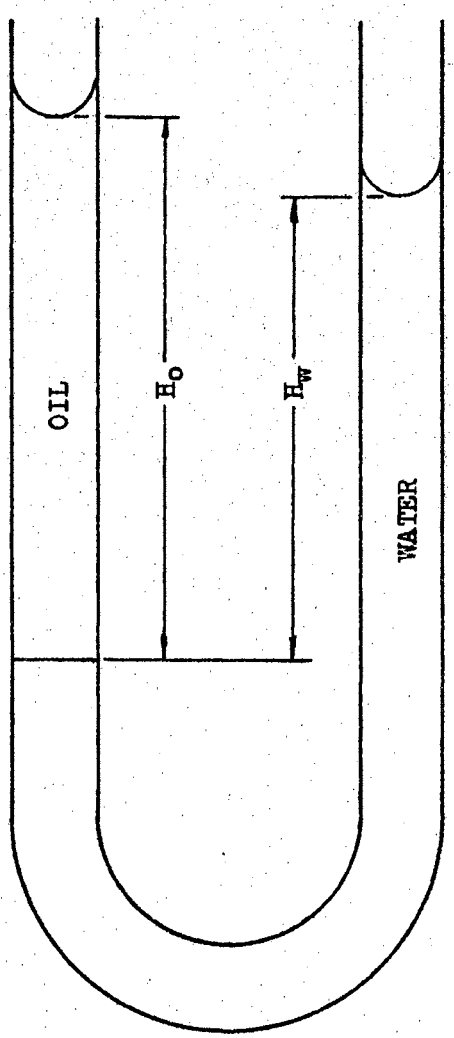

$$\frac{\rho_o}{\rho_w} = \frac{H_w}{H_o}$$

Figure 1. A Two-leg Manometer Used for Finding the Relationship Between the Density of the Calibration Oil and That of the Water Droplets

For every run made the oil remained at 78°F, so the following formula was found to relate the diameter of the droplet to its fall time (Δx_W = 0.391 inches):

$$d(\text{microns}) = 6352T^{-\frac{1}{2}} \text{ (sec.)}$$

where

$$(6352)^2 = \frac{\rho_L}{\rho_W} \frac{(1-\frac{\rho_Q}{\rho_L})}{(1-\frac{\rho_Q}{\rho_W})} \frac{\Delta x_W}{\Delta x_L} d_L^2 T_L$$

From this relation it is seen that this method of calibration is excellent for droplets 200 microns or larger but becomes prohibitively long for small droplets requiring about three hours to measure a 50 micron droplet.

The droplets, however, may be shown to remain spherical since the pressure inside the droplet is high and the pressure differential across it is low.

The pressure within a droplet due to the surface tension is

$$p = \frac{2S}{r}$$

where S is the surface tension in $\#_f$/in. and r is the radius of the droplet in inches. (Sears, 1958).

$$S = 4.10 \times 10^{-4} \text{ at } 78°F$$

$$r = 100 \text{ micron} \times \frac{1 \text{ in}}{25{,}400 \text{ micron}} = 3.94 \times 10^{-3} \text{ in.}$$

then $$p = \frac{2 \times 4.10 \times 10^{-4}}{3.94 \times 10^{-3}} = 0.208 \text{ psi}$$

Comparing this with the pressure differential in the oil from the top to the bottom of the droplet

$$\Delta P = \rho g \Delta h$$

ρg for the oil is $\frac{62.4}{1728}$ (0.895) $= 3.24 \times 10^{-2}$ #f/in^3; therefore

$$\Delta P = 2.55 \times 10^{-4} \text{ psi}$$

a hardly significant change considering that the droplet contains 1000 times this pressure. Similarly, if the droplet is resting on the bottom with all of its weight supported by its internal pressure and buoyant force, it is quickly seen that only a small amount of area is needed to support its weight. It was experimentally determined that the droplet does not wet the bottom and has no tendency to spread. The weight of the droplet is

$$W = 3.24 \times 10^{-2} \text{ \#f/in}^3 \times 4/3\pi(3.94 \times 10^{-3})^3$$

$$\text{Weight} = 8.25 \times 10^{-9} \text{ \#f}$$

$$\text{Buoyant force} = (.895)(8.25 \times 10^{-9} \text{ \#f})$$

and hence the force to be supported by the bottom is 8.67×10^{-10} #f. This would require an area of

$$A = \frac{8.67 \times 10^{-10}}{0.208} = 4.16 \times 10^{-9} \text{ in}^2$$

The radius of the supporting area would be

$$r = 3.64 \times 10^{-4} \text{ inches} = 9.25 \text{ microns}$$

which is 9.25% of the maximum radius. The volume displaced in supporting the droplet is 0.013% of the total volume; therefore, no distortion of the droplet can be detected. In view of these facts, it would be unreasonable to assume that the droplet, either falling or at rest on the bottom, was anything but spherical.

Observation has shown that the droplets have no tendency to run together either on the surface or when immersed in the oil. Apparently

the droplet is able to penetrate the surface but remains partially submerged, suspended by the surface tension of the oil. The oil film thus created between the droplets prevents two droplets from coalescing even though they may be in contact with one another. S. A. E. 30 oil readily accepts low velocity droplets into the surface thereby reducing the tendency for the droplets to bounce about on the surface.

The falling droplet method has a great advantage in that droplets of the same diameter fall at the same rate, and the uniformity in the size of a large number of droplets can be easily checked. For smaller droplets, the time required for this test is extremely long, and a shorter method had to be found.

Microscopic Method

Using the information gained by the drop fall method, it was then easy to use a microscope with an eyepiece grid calibrated in microns to determine droplet diameter. The droplets were first caught in a millipore filter dish in a 1/8-inch film of oil. These were quickly poured into a 10 ml graduate containing 10 ml of oil and covered with a drop of oil. This put the droplets under the oil permanently so that they would be preserved for prolonged handling and viewing. The droplets were then canted off from the graduate to another millipore filter dish and allowed to settle. The filter paper was in place in the second dish to facilitate the focusing of the microscope. After settling, the droplets were viewed and measured by a microscope with an eyepiece grid for fluid contamination studies.

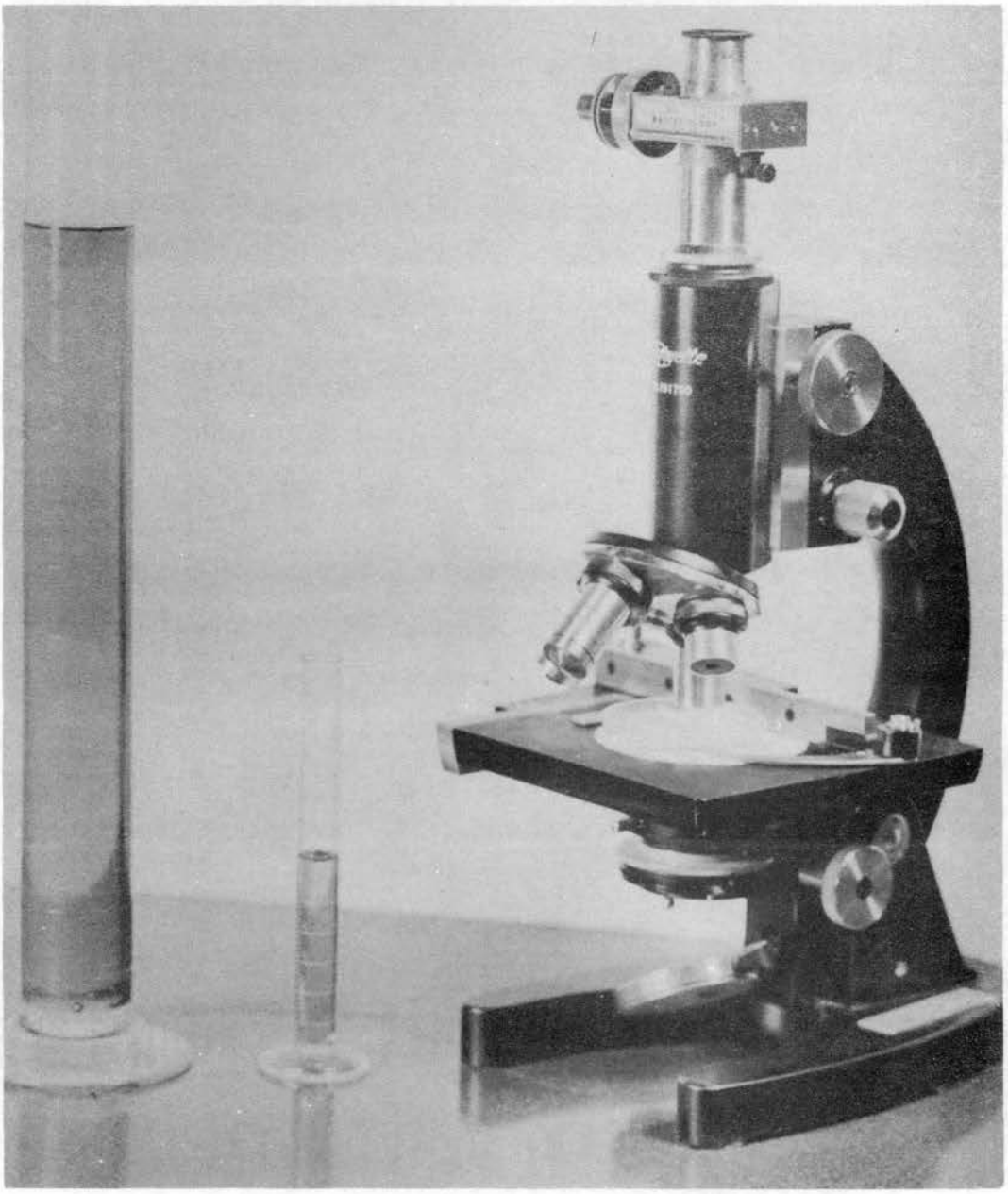

Figure 2. Droplet Measurement Equipment

The accuracy of this measuring method is unquestionable since the oil was first seeded with wires of known size which were microscopically checked. It has also been shown that due to the high pressure within the droplet and the comparison of densities of oil and water, the droplet remains spherical for all practical purposes even though it is resting on the bottom of the dish. This method provided a quick, accurate manner for studying the droplets produced in the following experiments.

DEFINITION OF SYMBOLS FOR CHAPTER II

V	steady state velocity of a sphere
Δx	distance traveled in time T
T	time for sphere to travel Δx distance
r	radius of the sphere
g	acceleration of gravity
μ	absolute viscosity
ρ	density of the sphere
ρ_o	density of the oil
d	diameter of a sphere
d_W	diameter of a water droplet
ρ_L	density of lead
ρ_W	density of the water droplet
d_L	diameter of a lead calibration sphere
Δx_W	distance traveled by water droplet during measurement time T_W
Δx_L	distance traveled by lead sphere during calibration time T_L
T_W	time for water droplet to travel Δx_W
T_L	time for lead sphere to travel Δx_L
p	pressure inside a droplet of radius r
S	surface tension
W	weight of the droplet

CHAPTER III

MECHANICAL METHOD OF DROPLET PRODUCTION

Physical Description

The author observed from previous trials with magnetically excited vibrating reeds of glass capillary tubing that the reed oscillated with a nonplanar motion. The predominant mode of oscillation was an elliptical path followed by the tip of the reed. The mechanical shaker shown in Figure 3 was designed specifically to produce a linear path.

The simple crank mechanism was designed as follows: Upon a one-half inch base was mounted three pillow blocks, two small and one large. The two small pillow blocks contained 11/16 inch O. D. ball bearings and were mounted in line to receive the vibrating shaft. Eight inches from this line and parallel to it was mounted the large pillow block containing a 1-1/8 inch O. D. ball bearing. This crank had an eccentric 1/4-inch diameter which was 3/8 of an inch off the crank's center and was driven by a 1/15 H. P. series wound electric motor. A connecting rod with a ball bearing on the crank end and a bronze bushing on the vibrating arm end connected the crank with the vibrating arm. The vibrating arm was 1-1/2 inches long and was joined to the vibrating shaft. The center of the crank was mounted at the same height as the pivot on the vibrating arm,

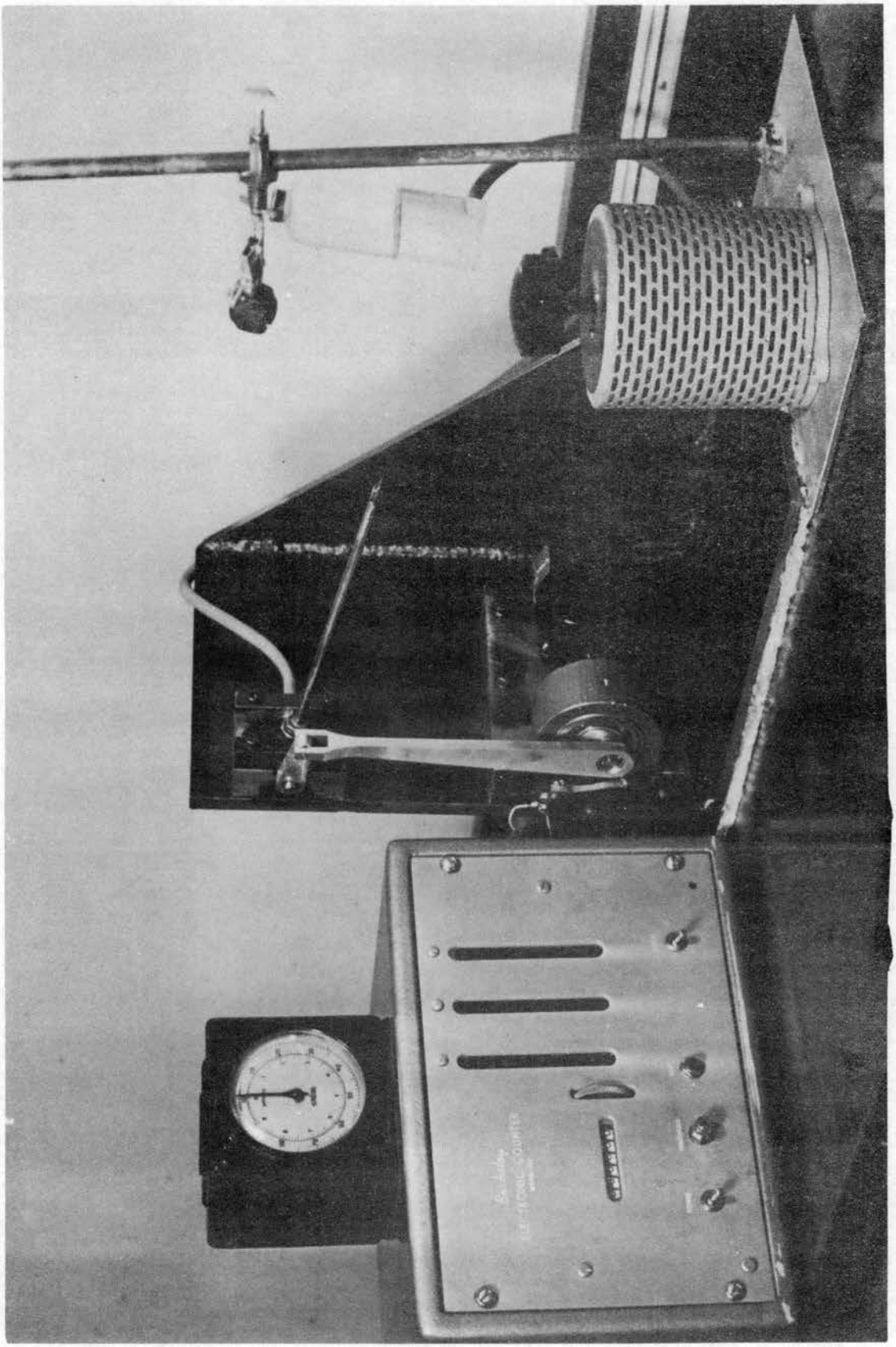

Figure 3. Mechanical Method Equipment

so that a sinusoidal motion of the arm would be closely approximated. The vibrating shaft had a 1/8 inch hole drilled half way down the axis from the side opposite the pinned joint. This hole was intersected by a threaded hole at right angles to it at the center of the shaft. The vibrating shaft was pressed into the bearings until the threaded hole was midway between them. This threaded hole received a bolt with a 1/8 inch hole drilled along its axis and countersunk 1/4 inch from the head end. Into the countersunk portion, a 1/4 inch stainless steel tube nine inches long was silver soldered, and upon this rod the tip was mounted.

The various tips used in this experiment were attached to the rod by a small aluminum insert epoxied into the end of the rod. This insert exactly fit the inside of a hypodermic needle base, and when ordinary canning wax was introduced between the needle base and the insert, the effect was to glue the needle to the rod. Ordinary canning wax proved to be very strong and replaced glue in most of the experiments since it was light, strong, and considerably quicker to apply than conventional glue.

The first hypodermic needle tried was a #26 Huber point, the closest one can buy to a side ejection needle, but its 0.007 inch I. D. was not sufficient to dissipate the tremendous pumping action produced by the oscillating rod, and the droplets were too large. Then pieces of 0.010 inch O. D. to 0.002 inch O. D. glass capillary of varying lengths were waxed into a #22 slant point needle, with most of the capillary extending down the stainless rod and only 1/8 inch exposed. This method of mounting the glass capillary was most effective

in preventing it from being plugged by miscellaneous particles in the water. A 0.010 inch O. D. capillary five inches long produced the smallest droplets, 300 microns in diameter.

Analysis

The mechanical shaker proved to be an excellent oscillating pump, being able to draw several feet of negative head and producing several feet of head on the pressure side. To demonstrate this point, consider a small element of water in the tube as in Figure 4.

$$\rho gHA - \rho gAR \sin \theta_V + \int_0^R r(\dot{\theta}_V)^2 dm = AP_{(t,R)}$$

$$dm = \rho A dr$$

$$\dot{\theta}_V = \theta_o \omega \cos \omega t$$

and assuming vibrations of less than 10°

$$\sin \theta_V = \theta_V$$

after evaluation

$$\frac{P(t)}{\rho g} = H - R\theta_o \sin \omega t + \frac{R^2 \theta_o^2 \omega^2}{2g} \cos^2 \omega t$$

This pressure is opposed by three things:

1. The inertia of the fluid. This is negligible since the only fluid being accelerated is that in the capillary, a very small quantity in comparison with the total head loss.
2. The internal pressure of the forming droplet.

$$P_B = \frac{K}{\left[\int_0^t \dot{Q}\, dt\right]^{1/3}}$$

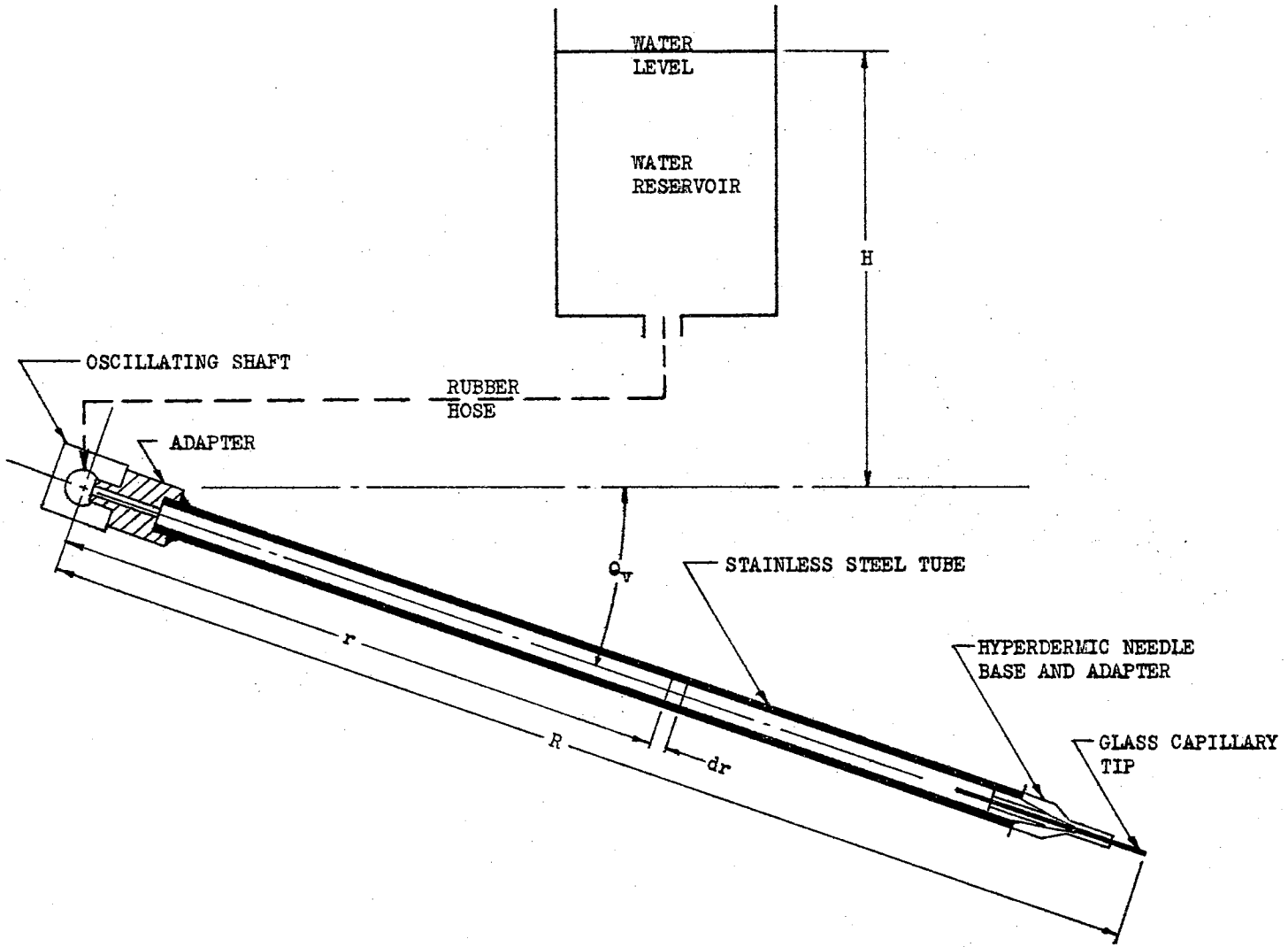

Figure 4. Detail Drawing of Vibrating Rod

This term is negligible since the drop never has a small enough radius to produce a significant back pressure.

3. And finally, the pressure drop through the capillary tip. This, for the sake of simplification, will be taken to be proportional to the mass flow rate. In short, Hagen-Poiseuille flow is assumed.

A slight digression is now in order since the flow will be neither turbulent nor laminar anywhere in this vibrating reed. There has been little work done in low Reynolds number flows in vibrating pipes, but the author has seen one such experiment carried out by Droste, Waters, and Weber (1961). In this experiment, low Reynolds number flow was induced in a lucite tube 10 feet long with a small stream of fluorescein dye down the middle of the flow so that turbulent regions could be easily found. A short section, about 1 foot of the tube was clamped at both ends to the table top, and the portion between the clamps was vibrated at varying speeds and amplitudes. Under moderate vibration, the dye stream would adopt a sinusoidal path for the full length of the tube. The more violent the vibration became the greater became the amplitude of the sine wave. Eventually the dye stream would come in contact with the tube wall and a spot of turbulence would be observed. Increasing the amplitude of the vibration caused the turbulent spot to grow until the entire stream became turbulent. No quantitative results were obtained from this experiment, but it seems to be an excellent argument against Hagen-Poiseuille flow in a vibrating reed.

Realizing that the flow was more complicated than Hagen-Poiseuille flow but that it remained mostly laminar, the author assumed, for the

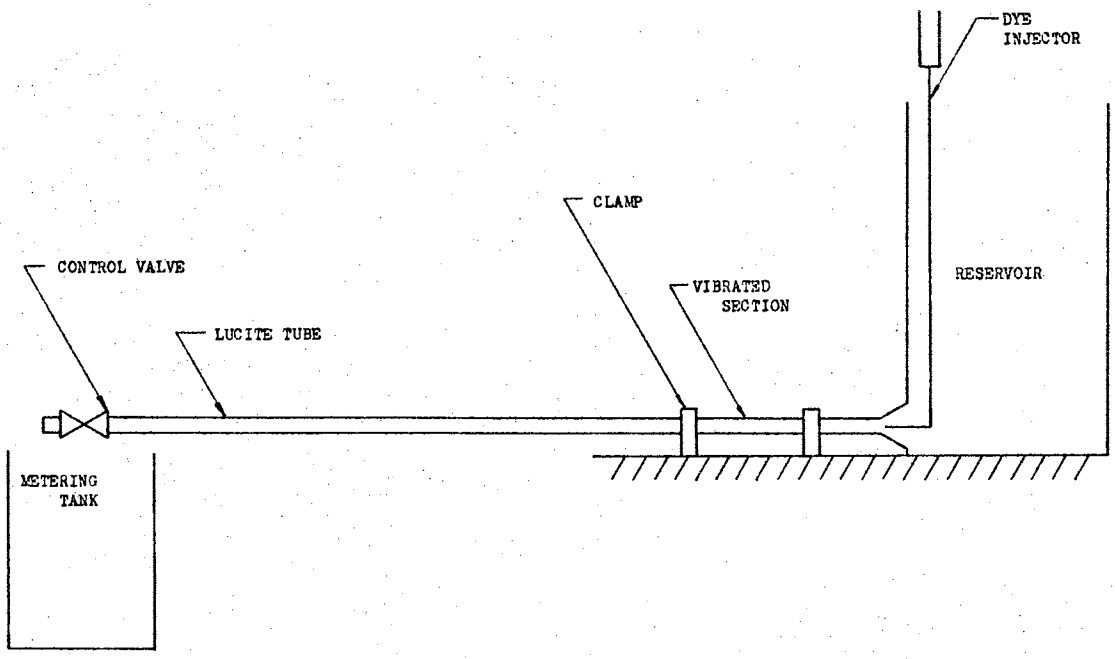

Figure 5a. Schematic of equipment used in experiment involving low Reynolds number flow in vibrating tubes.

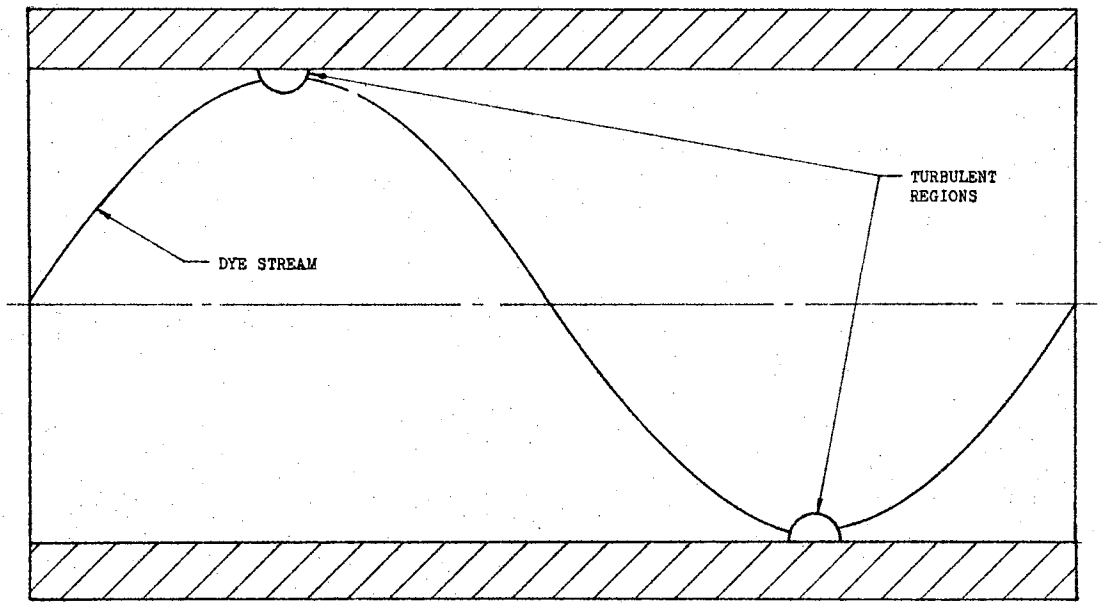

Figure 5b. A section of the downstream tube showing the effect of the vibrations upon the path of the dye stream.

Figure 5. A Schematic of an Experiment in Low Reynolds Number Flow in Vibrating Tubes

sake of analysis, that Hagen-Poiseuille flow existed.

$$C \frac{dm}{dt} = \frac{P(t)}{\rho g}$$

and integrating this from some initial t_o and m_o to a final t and m one finds that the mass of water on the end of the reed is

$$m = m_o + \frac{H}{C}(t-t_o) + \frac{R\theta_o}{C\omega} (\cos \omega t - \cos \omega t_o)$$

$$+ \frac{\theta_o^2 R^2 \omega}{2gC} \left[\frac{\omega}{2} (t-t_o) + \frac{\sin 2\omega t - \sin 2\omega t_o}{4}\right]$$

The force on the droplet at the end of the reed is

$$\vec{F} = m \left[R(\dot{\theta}_V)^2 + i\, R\, \ddot{\theta}_V\right]$$

then the absolute value of this force is

$$|F| = mR\theta_o\omega^2 \sqrt{\theta^2 \cos^4 \omega t + \sin^2 \omega t}$$

which is balanced by the maximum surface tension force

$$|F| = \pi\, d_o\, S$$

Finally, there is a droplet produced every time the maximum surface tension force is exceeded, so

$$S\pi d_o = \left\{m_o + \frac{H}{C} (t-t_o) + \frac{R\theta_o}{C\omega} (\cos \omega t - \cos \omega t_o)\right.$$

$$\left. + \frac{\theta_o^2 R^2 \omega}{2gc}\left[\tfrac{1}{2}\omega(t-t_o) + \frac{\sin 2\omega t - \sin 2\omega t_o}{4}\right]\right\}$$

$$\left\{R\theta_o\omega^2 \sqrt{\theta^2 \cos^4 \omega t + \sin^2 \omega t}\right\}$$

This is the total governing equation for the separation of the droplets. If at time t_o, m_o is the mass of water on the end of the rod

then the time t of droplet separation could be found. Repeating this procedure would produce the time of the next drop separation.

It is obvious from this equation, that there are two factors in the droplet separation problem; namely ω and H for a fixed time of separation, t. It is also not so obvious but nevertheless true that unless droplets are separated at precisely the correct moment they will neither travel the same path nor be of uniform size.

To produce droplets that are both uniform and travel in the same path as others, there must be separation at one of two places;

1. $\omega t = \frac{\pi}{2}$; $\omega t_o = -\frac{\pi}{2}$ (end separation) or

2. $\omega t = 0$ and $\omega t = \pi$ (center separation)

The angle at which the maximum acceleration occurs is solely dependent upon the value of θ_o . For values of θ_o greater than 0.75 radians, the maximum acceleration occurs at some angle of θ between zero and θ_o ; however, the θ_o used in the experiments presented in this paper was 0.3 radians which produced end separation as the prevalent mode. Even though other modes of separation are possible, this analysis was limited to end separation as observation proved it to be obtained with the lowest rpm.

Substituting in the values of ωt and ωt_o in the equation, one finds that

$$\frac{S\, d_o}{R\theta_o} = \frac{H\omega}{C} + \frac{\theta_o^2 R^2 \omega^3}{4gC}$$

giving the proper relationship between H and ω for all droplets to separate at the ends of the stroke. This shall be called the phasing

equation. Complementing this is the droplet equation which is found by

$$Q = \frac{m}{\rho}\Big|_{\omega t_o}^{\omega t} = \frac{\pi}{6} D^3 = \frac{\pi}{\rho C} \cdot \frac{H}{\omega} + \frac{\pi \theta^2 R^2 \omega}{4 g \rho C}$$

$$\text{or } D^3 = \frac{6}{\rho C} \frac{H}{\omega} + \frac{3}{2} \frac{\theta_o^2 R^2 \omega}{\rho g C}$$

Combining these equations the diameter of the droplets separated must then be

$$D^3 = \frac{3 \theta_o^2 R^2}{\rho g C} \omega - \frac{6 S d_o}{\rho R \theta_o} \frac{1}{\omega^2}$$

where $$C = \frac{128 \mu l}{\pi d_i^4 \rho^2 g}$$

Results

In the experiments carried out with this piece of apparatus, there was found to be a definite relationship between H and ω which exists for a steady end or center separation point. Since the equation is so sensitive to the values of the constants in it and the ω is limited by the maximum speed the motor can produce, the relationship between D and ω is rather difficult to check.

The droplets were extremely accurate in the path that they took, their point of impact being completely predictable (± 1/16 inch in one foot of travel) and completely reproducible.

There were several disadvantages, however, which offset the previously mentioned advantages. The major one of these was that the droplets were all too large, being in the range of 300 to 500 microns

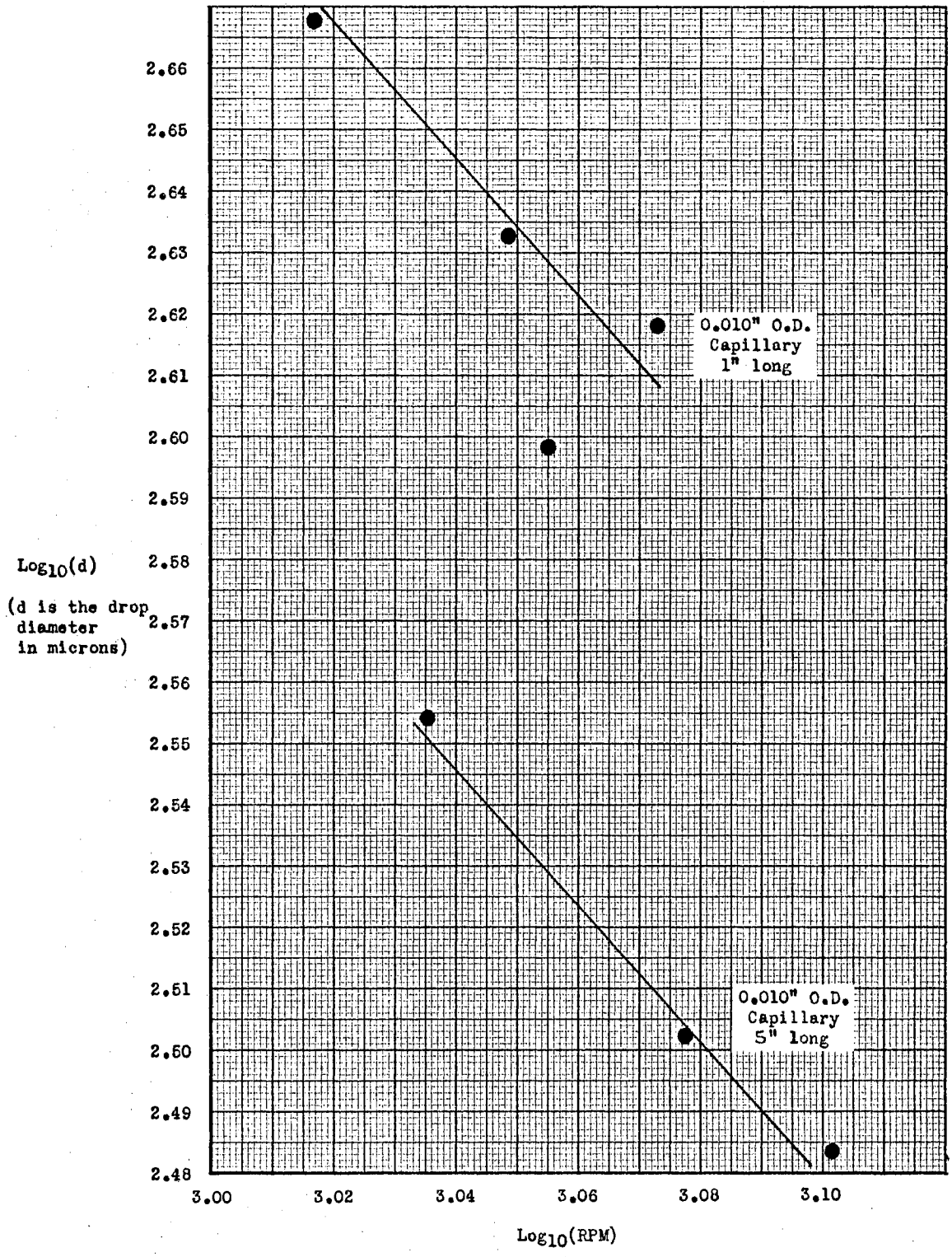

Figure 6. The Results of the Mechanical Method of Droplet Production for Two Different Capillary Tips

in diameter. The theory presented previously shows that the droplet size for a given frequency may be reduced by increasing the capillary constant, C, and hence reducing the flow rate for a given head and pumping action. This was demonstrated with great success by numerous tries with smaller and longer capillaries. There is a point, also noted from the theory, that is the cut-off point; i. e. there is a frequency at which end separation for every stroke begins and exists for every frequency higher than that. Lower rpms from the critical cut-off rpm will not produce any regular pattern or droplet separation. It is the author's opinion, from observation, that for the larger C values tried the motor would not produce a frequency above the cut-off frequency. After the experiments were run, some trial calculations were made, and it was found that the cut-off frequency was some three times the produced speed.

While the reed had a very simple motion at low speeds, it was found that lateral vibrations in the reed appeared at higher speeds producing a droplet stream that was not in the plane of the reed's major vibration. The later vibrations were as high as the fourth natural frequency and produced uneven loading on the trunions thereby causing erratic operation of the motor.

DEFINITION OF SYMBOLS FOR CHAPTER III

ρ the density of water

g the acceleration of gravity

A cross sectional area of the stainless steel tube

ω radian frequency of oscillation of the stainless steel rod

H the static head

t time

θ_o maximum angle that the stainless steel tube makes with the horizontal

$\dot{Q}$ flow rate through the glass capillary

C the Hagen-Poiseuille constant for flow in units mass per unit time

t_o initial time

m_o mass on end of capillary at initial time

S surface tension

d_o outside diameter of glass capillary

d_i inside diameter of glass capillary

D diameter of the separated droplet

CHAPTER IV

THE ELECTRO-MECHANICAL PRODUCTION OF DROPLETS

Power Dissipation

Due to the inability of the mechanical method to achieve a high enough frequency for small droplet production, the electro-mechanical method was then retried with some changes since this method may achieve any frequency desired. The vibration of large tubes was immediately ruled out because of the enormous amount of power necessary to vibrate them. In hysteresis loops, it is generally accepted that

$$\frac{dE}{dV} \cong C\sigma^{1.8}$$

where E = the energy dissipated

V = the volume undergoing strain

σ = the stress on that volume. (Gray, 1955)

For the sake of simplicity, let

$$dE = C\sigma^2 dV$$

but $$dV = dAdl$$

and from simple moment bending

$$\sigma = Kyf_{(l)} \qquad (K \text{ is a constant})$$

$f(l)$ equals the loading function of the rod as a function of length; then

$$dE = CK^2y^2f^2_{(l)}dAdl$$

and rearranging

$$dE = CK^2y^2dA\ f^2_{(l)}dl$$

By integrating this over the volume of the beam, the energy dissipated in bending is

$$E = \int_0^E dE = CK^2\int_0^l f^2_{(l)}\left[\int_0^A y^2dA\right]dl$$

and recognizing $\int_0^A y^2dA$ as $I_{(l)}$ the second moment of area as a function of length, then

$$E = CK^2\int_0^l I_{(l)}f^2_{(l)}dl$$

or for a constant area rod

$$E = CK^2I\int_0^l f^2_{(l)}dl \qquad \text{per vibration.}$$

Hence, for round rods about 1/4 inch in diameter, this rough approximation assumes that the energy dissipated increases and becomes much too large to excite them advantageously with magnets. The power dissipated in the rod is a minute fraction of the total power dissipated by the magnet, but any increase in the rod's power dissipation requires a similar increase in magnetic flux. This increase creates very large expenditures of power by eddy current losses in the magnet core. Therefore, the prohibitive power dissipation stems directly from the core of the magnet but indirectly from the dissipation in the rod.

The unavailability of a better magnet left only small reeds available for magnetic vibration. As a capillary tube vibrates in a planar

motion, any small irregularity will cause it to oscillate sideways, and the tip will then follow an elliptical pattern. The primary source of such side motions develops from the cylindrical tube moving through the air. This produces an effect similar to swinging a broomstick in water, and hence the start of side vibrations. Once the side vibrations have started, they increase until a steady state ellipse is reached.

The first method of eliminating the side motion of the reed was to try putting guides somewhere on the vibrating portion to force the tube to follow a planar motion. This has a serious disadvantage in that the guides, to be effective, must be tight enough on the tube so as to force the tube into a planar motion. The frictional forces produced by this tightness will destroy the entire vibrational structure which is necessary for inducing the maximum vibration of the tube. Loosening the guides only slightly will allow the reed to strike the sides thereby producing erratic side vibrations rendering the reeds even more useless than the single tube.

Multiple Capillary Tubes

It was ascertained from these facts that to get a simplified motion from a reed the natural frequency in one direction must be different from the natural frequency in a perpendicular direction. To do this the second moment of area in one direction must be different from that of the direction perpendicular to it. Unfortunately, elliptical and rectangular glass tubing is not made commercially, but two or more glass tubes may be welded together to produce the desired result.

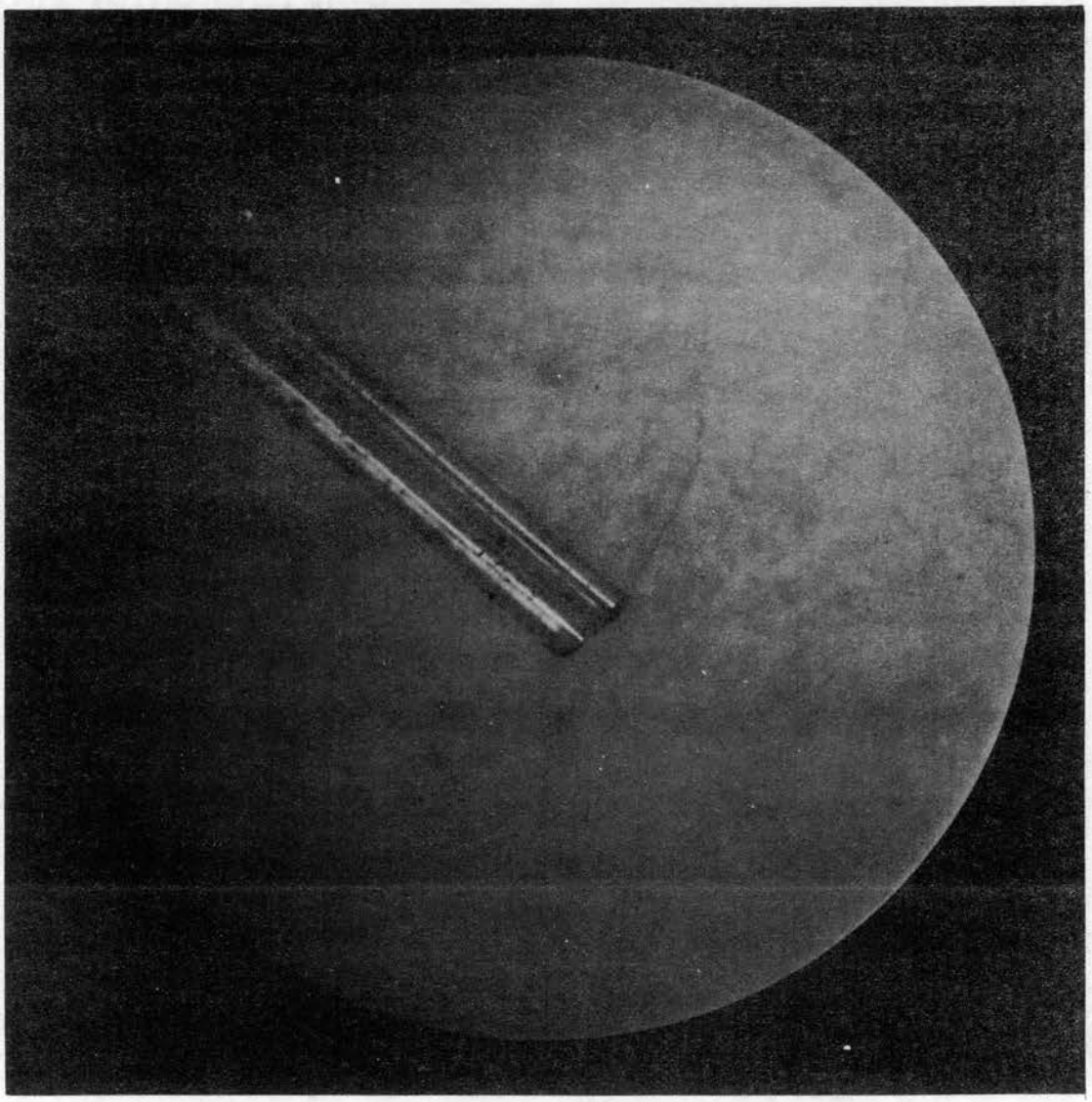

Figure 7. A Dual Glass Capillary (x25)

With a little practice, two glass tubes were softened in the flame of a grid burner, and a joint was made between them along their sides. Then the tubes were softened enough to draw them in the usual manner of producing a capillary tube. The result was a double capillary tube, both sides being perfectly round and having a joint entirely down their length. One of these capillaries was then reduced in length by placing a blade on the tip end with the end of the blade resting on the joint. With a quick downward thrust, about 1/4 inch of one capillary was crushed at the tip. The resulting tube had the vibrational properties of the two joined tubes but afforded only one tube on which the surface tension of the droplet might act.

One of the difficulties encountered in the production of these tubes was that the joint between the tubes was about 0.005 inches wide. This joint did not seem to reduce as the tubes were drawn into 0.005 inch diameter capillaries, and these capillaries were found to be inseparable. This inseparability was the result of the joint extending from the top to the bottom of the capillaries which solidly joined them. The advantage of fine tubes over large capillaries, the reduction of glass surface to which the droplet might adhere, was sacrificed to the simplicity of motion requirement, and thus only certain sized multiple capillaries were able to be produced with success.

Thermal stresses set up in the base of the capillary tended to make the larger portions, necessary for the introduction of water through a rubber tube, shatter or break off. In these cases, another base was waxed onto the capillary with ordinary canning wax so that water could be introduced for drop production.

In multiple capillary reeds the natural frequency in one direction is never changed while the natural frequency of the perpendicular direction is changed radically from the single tube value. The primary vibratory direction will be referred to as the y-direction, and the secondary direction, perpendicular to the primary direction, will be the x-direction. The problem in this method of securing motion simplicity was to keep the x-natural frequencies considerably different from all of the y-natural frequencies so that when the tube was vibrating at a y-frequency any accidental excitation in the x-direction would not be in resonance with one of the x-frequencies. If this condition were obtained, the excitation would be damped out, and the motion would remain simple and planar.

The multiple capillary reeds were vibrated primarily at the second natural frequency; hence the relation of the second y-frequency was investigated with relation to the first x-frequency. The second x-frequency was eliminated immediately when more than one capillary was present, since it became about three times as large as the second y-frequency.

Let $f_2(2y)$ mean "the second natural frequency of a two tube capillary in the y-direction" and $f_1(2x)$ mean "the first natural frequency of a two tube capillary in the x-direction." Then these relationships are cited:

$$\frac{f_2(2y)}{f_1(2x)} = 2.80 \qquad \text{(two tubes)}$$

$$\frac{f_2(3y)}{f_1(3x)} = 1.84 \qquad \text{(three tubes)}$$

$$\frac{f_2(4y)}{f_1(4x)} = 1.365 \qquad \text{(four tubes)}$$

$$\frac{f_2(5y)}{f_1(5x)} = 1.09 \qquad \text{(five tubes)}$$

It is immediately seen that with five tubes side by side the tip would again describe an ellipse; therefore, multiple capillary vibrating reeds must be limited to having from two to four tubes if excited at the $f_2(y)$ frequency.

Two side by side tubes produced best results by experiment; therefore, these were used. The elements of the theoretical analysis would be identical to the previous mechanical analysis; that is, there would be a pumping action and a static head to be opposed by the capillary head drop, the droplet back pressure, and the inertia of the water column. The surface tension and droplet size governs the droplet separation point as a phasing equation. The ω would be fixed since all experiments were made at 120 cps. and the phasing equation would relate the amplitude of the vibration to the static head, H.

It was found in the experiments that there was a definite relation between the amplitude of vibration and the static head. The motion of the reed was planar, and the separated droplets followed the same path in the plane of vibration. Accuracy was excellent, but as in the case of the mechanical method, the frequency was too low and 250 micron droplets were the smallest obtained directly. As each 250 micron droplet was separated from the reed, a small 50 micron droplet was formed from

the water connection between the large droplet and the reed. These small droplets also formed a stream thereby producing four streams, one large and one small at each end of the reed's stroke. There was no apparent way of controlling this small stream for size so this method of droplet production was also abandoned.

The Vibrations of a Constant Cross Sectional Cantilever Beam

A brief review of the theory involving the vibration of a cantilever beam is in order here. It is imperative that the coupling between any magnetic driving source and the beam be made at an antinode on the beam. Hence, the investigator must be able to locate the nodes and antinodes for whatever beam is being used rapidly so that the coupling to the magnetic driving source may be placed immediately without any loss of experimentation time. The analytical methods of locating nodes and antinodes presented in this paper are approximate but are used in the interest of rapid calculation.

The solution for the general mode shape of a freely vibrating cantilever beam of constant cross section is:

$$Y = \sum_{\lambda_1}^{\lambda\infty} An\Big[(\sinh Z_n + \sin Z_n)\Big\{\cos\Big[Z_n(\tfrac{X}{l})\Big] - \cosh\Big[Z_n(\tfrac{X}{l})\Big]\Big\}$$

$$- (\cosh Z_n + \cos Z_n)\Big\{\sin\Big[Z_n(\tfrac{X}{l})\Big] - \sinh Z_n(\tfrac{X}{l})\Big]\Big\}\Big]\Big[\sin \lambda nt\Big]$$

where $Z_n = \sqrt{a}^{\lambda n}\ l$. (Wylie, 1951).

Z_n is determined by the Eigen equation, and for the pure second node $Z_2 = 4.693$. The mode shape of this solution is presented in Figure 8.

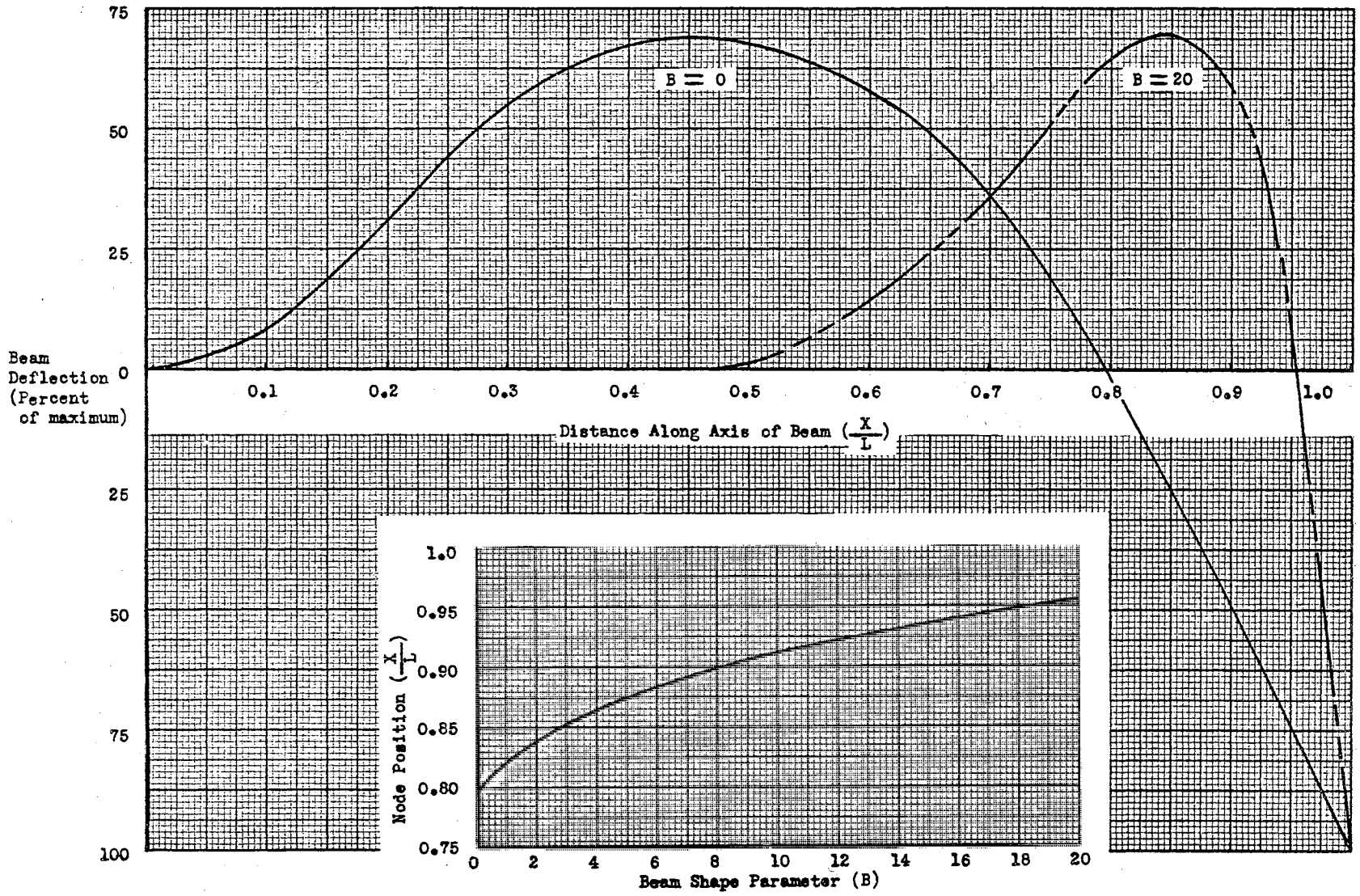

Figure 8. Vibrational Modes of Non-uniform Cross Sectional Cantilever Beams With $A = A_o e^{\frac{-Bx}{L}}$ Plotted for Two Values of B

(Insert plots the x dependence of the node position as a function of beam shape).

This solution omits all of the real complications to the problem such as corrections for rotational inertia, damping, and the effect of point loading by the magnetic driver; however, it seems to be accurate enough to provide rapid information on the position of the nodes and antinodes.

Non-constant Cross Sectional Tubes

Experiments with constant cross sectional tubes indicated that the frequency was still too low. Higher frequencies were tried, but the amount of power necessary to produce vibration increased prohibitively. It was then noticed that a reed of non-constant cross section (a large cross section at the fixed end exponentially decaying to a small cross section at the free end) would produce violent vibrations with a very small power input. The principal reason for this is that the larger fixed end does not vibrate perceptibly as all of the vibration and power dissipation occurs near the free end. It was then necessary to have an analysis rapidly providing the position of the nodes and antinodes of a non-constant cross sectional cantilever beam.

The differential equation for small vibrations of a cantilever beam of non-constant cross section is:

$$\frac{\partial^2\left[EI_{(x)}\frac{\partial^2 y}{\partial x^2}\right]}{\partial x^2} = -\frac{\rho A(x)}{g}\frac{\partial^2 y}{\partial t^2}$$

If any regular polygon cross section is considered, then the $I_{(x)}$ is proportional to the square of the $A(x)$. For a round rod,

$$I(x) = \frac{1}{4\pi} A^2(x) \quad .$$

Furthermore, if the cross sectional area is assumed to be related to x by

$$A_{(x)} = A_o \, e^{\frac{-Bx}{L}}$$

where L = length of the rod, this closely approximates the shape of a capillary tube drawn from a larger glass tube.

By separating variables in the standard fashion and applying these last two relations for the I and A of the rod, the equation becomes

$$y = X_{(x)} \, T_{(t)}$$

$$A^2X^{IV} + 4AA' \, X^{III} + 2\left[A''A + (A')^2\right]X^{II} - \frac{4\pi\rho A\lambda^2}{Eg} \, X = 0$$

where λ is the Eigen function and A is the $A_{(x)}$.

For the simplification of the solution, shear, moment, and slope terms must be dropped from the equation leaving

$$A^2X^{IV} - \frac{4\pi\rho A\lambda^2}{Eg} \, X = 0$$

Next, if $X_{(x)}$ is considered to be $X\left[Z_{(x)}\right]$, then the transformation

$$Z = \frac{4}{(A_o)^{\frac{1}{4}}\left(\frac{B}{L}\right)} \left[e^{\left(\frac{B}{4}\right)\left(\frac{x}{L}\right)} - 1\right]$$

transforms the equation into

$$X^{IV}_{(Z)} - \frac{4\pi\rho\lambda^2}{Eg} \, X = 0$$

which may be solved conventionally as the constant cross sectional beam was solved, having the boundary conditions which follow.

$$X_{(x)}\Big|_{x=o} = 0$$

$$X^{I}_{(x)}\Big|_{x=o} = 0$$

$$X^{II}_{(x)}\Big|_{x=1} = 0$$

$$X^{III}_{(x)}\Big|_{x=1} = 0$$

The solution of this equation is related to the solution of the constant cross section equation by the transformation Z. Hence, as in the previous case, the solution becomes

$$X_{n(x)} = (\sinh Z_n + \sin Z_n)\left\{\cos\left[Z_n\left(\frac{Z}{Z_1}\right)\right] - \cosh\left[Z_n\left(\frac{Z}{Z_1}\right)\right]\right\}$$

$$- (\cosh Z_n + \cos Z_n)\left\{\sin\left[Z_n\left(\frac{Z}{Z_1}\right)\right] - \sinh\left[Z_n\left(\frac{Z}{Z_1}\right)\right]\right\}$$

where $$Z_n = \sqrt[4]{\frac{4\pi\rho}{EgA_o}}\ \sqrt{\lambda n}\ \left[\frac{4l}{B}\left(e^{B/4} - 1\right)\right]$$

and $$Z = \frac{4l}{B(A_o)^{\frac{1}{4}}}\left[e^{\left(\frac{B}{4}\right)\left(\frac{x}{l}\right)} - 1\right]$$

$$Z_1 = \frac{4l}{B(A_o)^{\frac{1}{4}}}\left[e^{\frac{B}{4}} - 1\right]$$

And Z_n is found from the Eigen equation as before. In fact, Z_2 still has the same value, 4.693, leading to the solution plotted in Figure 7. It will be noted that the constant and non-constant cross sectional rods have basically the same solution, but that the deflection values occur at different points on the $\frac{x}{l}$ scale. The relation between these $\frac{x}{l}$ values is, of course, the transformation $\frac{Z}{Z_1}$.

To plot the mode shape of the non-constant cross sectional case from the data of the constant cross sectional case, one needs only to find the value of $\frac{Z}{Z_1}$ for a given $\frac{x_N}{l}$, where the N means "non-constant cross sectional rod." The value of $\frac{Z}{Z_1}$ is then found on the $\frac{x}{l}$ scale for the constant cross sectional case, and the deflection at that point is noted. This deflection, then, is plotted versus $\frac{x_N}{l}$, and the series of these points from $\frac{x_N}{l} = 0$ to $\frac{x_N}{l} = 1$ is the solution for the non-constant cross sectional case.

The solution as found in the preceding manner and presented in Figure 8 gave excellent results for the location of the nodal points but the deflection values were not checked. Obviously, the neglected terms have a great deal to do with the deflection but change the nodal point only slightly. The reed would probably not adopt the solution's mode of bending because of the large bend in the end portion of the reed. Inaccurate as it may be, the solution of this equation gives some insight into the vibrations of a cantilever beam of non-uniform cross section.

Physical Description

A reed with a free end diameter of 0.010 inches was drawn from a thin-walled glass tube having a diameter of one-quarter inch. The large end was inserted into a rubber tube through which the static head was applied. The reed was then clamped in a horizontal position by the large end so that the clamps touched only the top and the bottom of the tube with no support being given to the sides as shown in Figure 9. A radio speaker diaphragm was connected face up to the

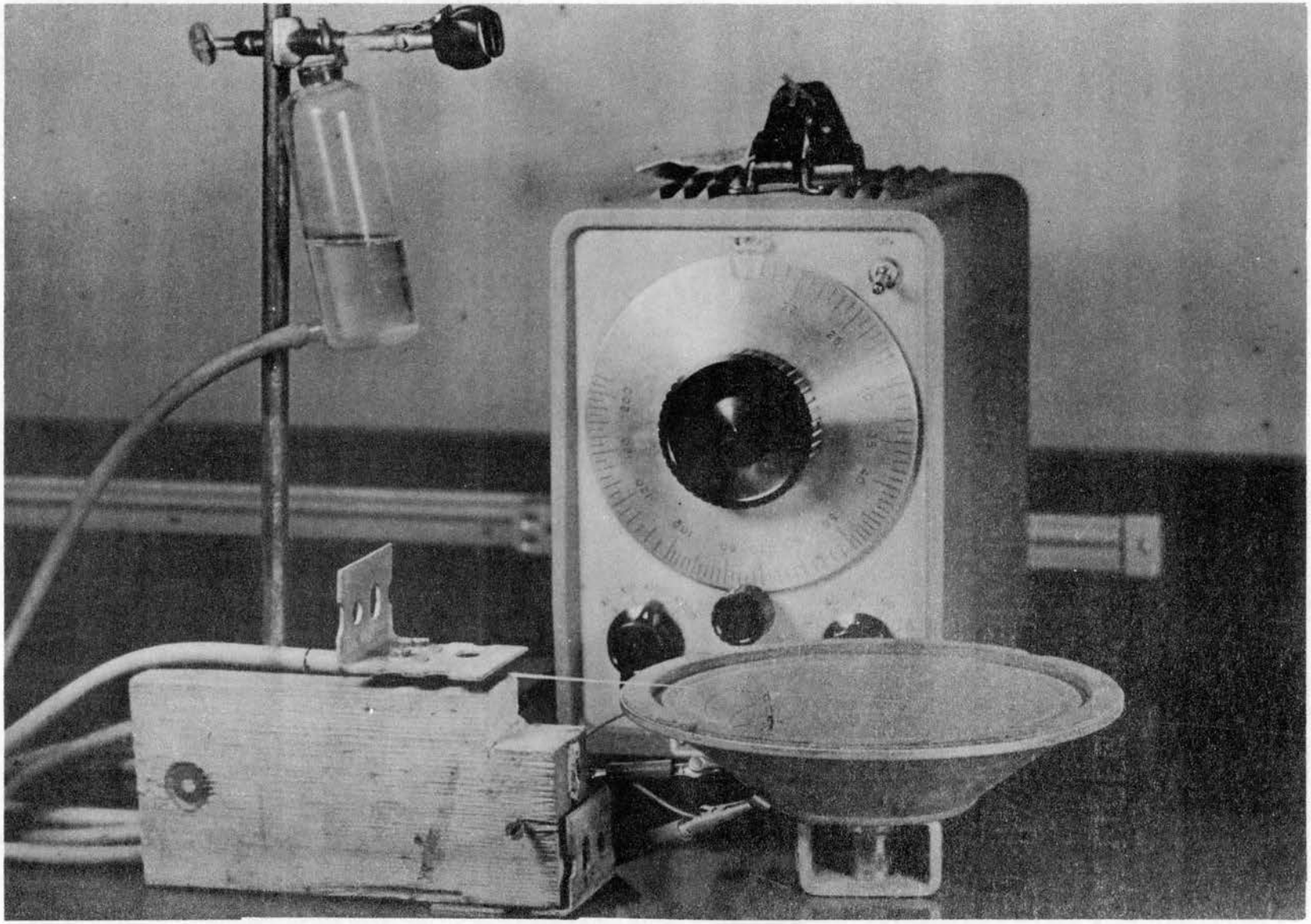

Figure 9. Electro-Mechanical Production Equipment

reed by means of a thread and a drop of wax. The connection was made near the middle of the reed to facilitate a maximum of response with a minimum of input amplitude.

Results

Due to the better coupling between the magnetic driving member and the reed, considerably less than a one-watt input, as opposed to 300-watts for the constant cross sectional reed, caused the reed to oscillate violently. It was extremely sensitive to the boundary conditions, and the mode of oscillation could be easily controlled by applying slight pressures to the large end of the reed where there was essentially no vibration. Guide rails or adjustment screws in this region would be highly effective in directing the mode of oscillation.

At 2000 cps., the mode of oscillation was planar, and the vibration was violent enough to produce a stream of 100 micron droplets all in the same trajectory. When the static head was changed, the droplets sprayed aimlessly from the ends of the stroke. With some adjustment to the frequency and amplitude, the stream was regained with only a minor change in the diameter of the droplets. This procedure was repeated until, at two feet of negative head, the pumping action was overcome and the water receded from the tube.

The analysis of the droplet stream thus produced is the same as before with the same factors being prominent. Again there is a relation between the amplitude, frequency, and static head for the stream to have

a stable separation point. In all three methods used to form droplets there was a very large pumping action present. It was not uncommon for the vibrating reeds to draw two feet of suction head and for the mechanical method to draw four feet. In this case, however, the surface tension tended to draw the water up the outside of the tube, and hence the droplet was formed from the outside, not the end of the tube.

Because of this adherence to the outside of the tube, the droplet was thrown in the opposite direction from the position that the tube occupied. As the reed decelerated toward the end of the stroke, the water on the tube sloshed into a droplet pointing toward the end of the stroke. The reed came to a rest, but the droplet remained moving. To remain in contact with the reed, the droplet must then have negotiated a corner with a very small radius. In turning the corner, the centrifugal force exceeded the surface tension force, and the droplet was separated.

In the author's opinion this seems to be the best method of producing the variable sized droplets in a given direction since the theory presented indicates different sized droplets might be produced by varying the head and amplitude.

DEFINITION OF SYMBOLS FOR CHAPTER IV

E	Young's modulus
I	the second moment of area
ρ	density of beam
y	deflection of the beam
x	distance along the beam axis measured from the fixed end
A	cross sectional area of the beam
A'	$\frac{dA}{dx}$
A''	$\frac{d^2A}{dx^2}$
X^{II}	$\frac{d^2X}{dx^2}$
X^{III}	$\frac{d^3X}{dx^3}$
X^{IV}	$\frac{d^4X}{dx^4}$
λ	Eigen function

CHAPTER V

INTERPRETATION OF RESULTS

Summary and Conclusions

There were several significant techniques found as a result of this study. One such technique was the microscopic display of the small droplets in oil in which they may be readily observed and measured. The use of this technique will enable future investigators to make rapid evaluation of the progress of their experiments and should reduce the amount of time necessary to find the solution to the problem.

Another technique that may prove useful to future investigators is the use of multiple capillaries as vibrating reeds. This author was unable to produce a multiple capillary straight enough to be used as a non-constant, cross sectional cantilever beam. Neither could the multiple capillaries be produced without the bases breaking off; however, this might prove to be a better method of obtaining planar motion than the single capillary.

The understanding of the mechanics of vibration and droplet formation is essential to the prediction of results. The discovery of the large pumping action associated with these vibrating reeds should prevent future analysts from excluding this as negligible, thus making a sizable error in the relationship between droplet size and frequency.

Although there were no quantitative results to the case of the vibrating non-constant, cross sectional reed, it seems evident that the same philosophy of analysis used on the mechanical method should be applied here. The pumping action will be much more difficult to evaluate because of the complicated mode shape, but it is essential to the analysis that it be solved. The definite trends suggested by the results of the mechanical experiment suggest that a droplet size to frequency relationship probably exists for the more difficult electro-mechanical case.

Finally, the solution presented in this paper for the mode shapes of vibrating non-constant, cross sectional cantilever beams appears to be fairly accurate for locating nodes even though it is an approximation. The rapid location of these nodes should reduce the time necessary for mounting a reed for vibration, and hence speed up experimentation. With these approximated mode shapes, the future analyst will have at his disposal a method of obtaining an approximate closed solution for the important pumping action term in his analysis. In any event, he should have a better understanding of the mechanics of the vibration so that he will be able to control the reeds successfully.

Implications of the Study and Suggestions for Future Study

This study has developed some very interesting sidelights in fluid flow and vibrational analysis. The experiment presented within this paper on "Low Reynolds Number Flow in Vibrating Tubes" could well become a doctor's thesis because of its complexity and obscurity. Due to the laminar flow property, the author intuitively feels that an application of this principle to the heat transfer field might well

produce compact heat exchangers with a high heat transfer rate per unit tube length at the expense of a very low pressure drop. It should be very interesting to hear an explanation of why the turbulent regions become laminar again instead of continuing as a turbulent boundary layer for the rest of the pipe's length. More experiments with an apparatus similar to the schematic in this paper might produce answers to these questions.

The analysis of the non-constant, cross sectional cantilever beam presented in this paper could be the basis for a master's thesis delving more deeply into the problem. This analysis lends itself to all beams having regular polygons as cross sections and analytical expressions for the area as a function of length, not just the exponential shape presented here. If some method were devised to handle non-analytical shapes and cross sections and produced the higher frequency mode shapes, it would be a great boon to the field of vibrational analysis. A more intensive study of correlations between actual and theoretical mode shapes and node positions would be in order to find the extent of validity of the presented analysis.

In extending the findings of this paper, it is suggested that future experiments begin with Chapter IV and study more closely the correlation between the static head and the diameter of the droplets produced. Repeating this for a large number of single reeds may produce the techniques and correlations necessary to solve the problem. Realizing that the phasing of the droplet formation plays an important role in the droplet separation will help to give the future investigators a feel of what is happening and perhaps a mode of controlling it.

The radio speaker method of stimulating vibrations has been the most successful, but it is a trifle wearing on the experimenter's ears. Some method, such as slitting the diaphragm or putting cotton in it, should be devised if a long series of studies are to be undertaken.

Horizontal reeds were used exclusively throughout the experiments with the intention of producing droplet streams that were vertical. The falling pattern of droplets is then independent of the velocity with which the droplet separates. Horizontal droplet streams have a trajectory that is dependent upon the separation velocity and the viscous air drag. Even though the turbulence of the air in a room is very slight, one person breathing or an air conditioner far away will cause enough turbulence so that the horizontal droplet stream will wander indiscriminately. Future experimenters should use long horizontal reeds, about 14 to 18 inches, in some plexiglass enclosure to prevent this effect.

BIBLIOGRAPHY

Church, Austin H. Kinematics of Machines. New York: John Wiley and Sons, 1956.

DeJuhasz, Kalman J. Spray Literature Abstracts. New York: American Society of Mechanical Engineers, 1959.

Dimmock, N. A. "The Controlled Production of Streams of Identical Droplets." National Gas Turbine Establishment (England). Memo M-115. 1951.

Dimmock, N. A. "Production of Uniform Droplets." Nature (England). Vol. 166. 1950.

Droste, C. S., L. Waters, and R. Weber. Inducement of Turbulence at Low Reynolds Number in Vibrating Pipes. Undergraduate report. Mechanical Engineering Department, Rice University. Houston, Texas. 1961.

Gray, Alexander, and G. A. Wallace. Principles and Practice of Electrical Engineering. New York: McGraw-Hill Company, 1955. pp. 69-71, 164-166, 368-370.

Higdon, Archie, and William B. Stiles. Engineering Mechanics. Englewood Cliffs, New Jersey: Prentice-Hall, Inc., 1955. pp. 209-256.

Keenan, Joseph H., and Frederick G. Keyes. Thermodynamic Properties of Steam. New York: John Wiley and Sons, 1958.

Parker, Jerald D. Heat Transfer to a Mist Flow. Thesis submitted to Purdue University as requirement for Ph. D., 1961.

Sears, F. W., and M. W. Zemansky. University Physics. Reading, Mass.: Addison-Wesley Publishing Company, 1956. pp. 224-255.

Skilling, H. H. Electrical Engineering Circuits. New York: John Wiley and Sons, 1958.

Slykhouse, T. E. and J. L. York. Uniform-Drop-Generator Method for Calibrating Spray Analyzer. 1886: 1-1-P. Engineering Research Institute, University of Michigan, July, 1954.

Streeter, Victor L. Fluid Mechanics. New York: McGraw-Hill, 1958. pp. 8-10, 145-150.

Strutt, John William and Baron Rayleigh. The Theory of Sound, Vol. II. New York: MacMillan and Company, 1896. pp. 360-365.

Thaler, George J. and Robert G. Brown. Analysis and Design of Feedback Control. New York: McGraw-Hill Company, 1960.

Wylie, C. R., Jr. Advanced Engineering Mathematics. New York: McGraw-Hill Company, 1951. pp. 199-234, 482-488.

3-M Surfactant for Reducing Surface Tension of Water 100 Times Better Than Other Surfactants. 3-M Chemical Division, Department KAK-61, Minnesota Mining and Manufacturing Company. St. Paul 6, Minnesota.

APPENDIX

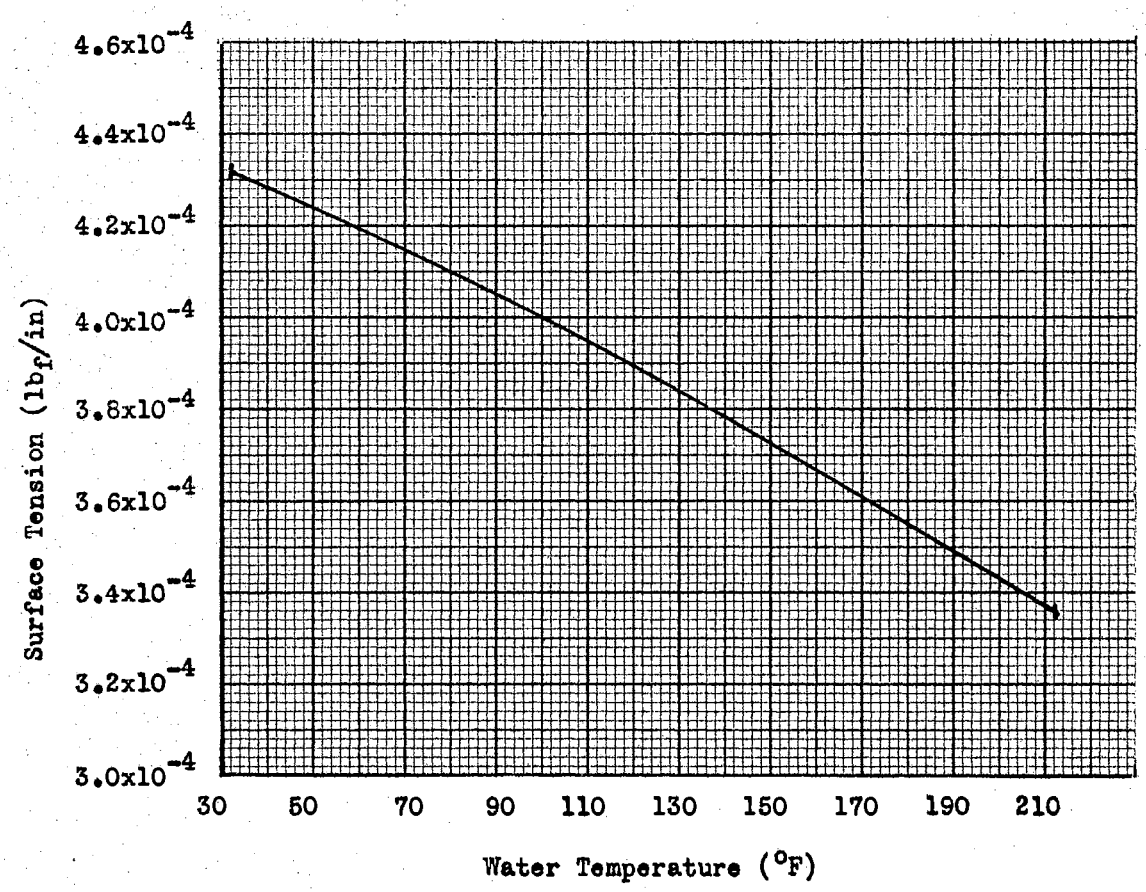

Figure 10. The Effect of Surface Tension of Water

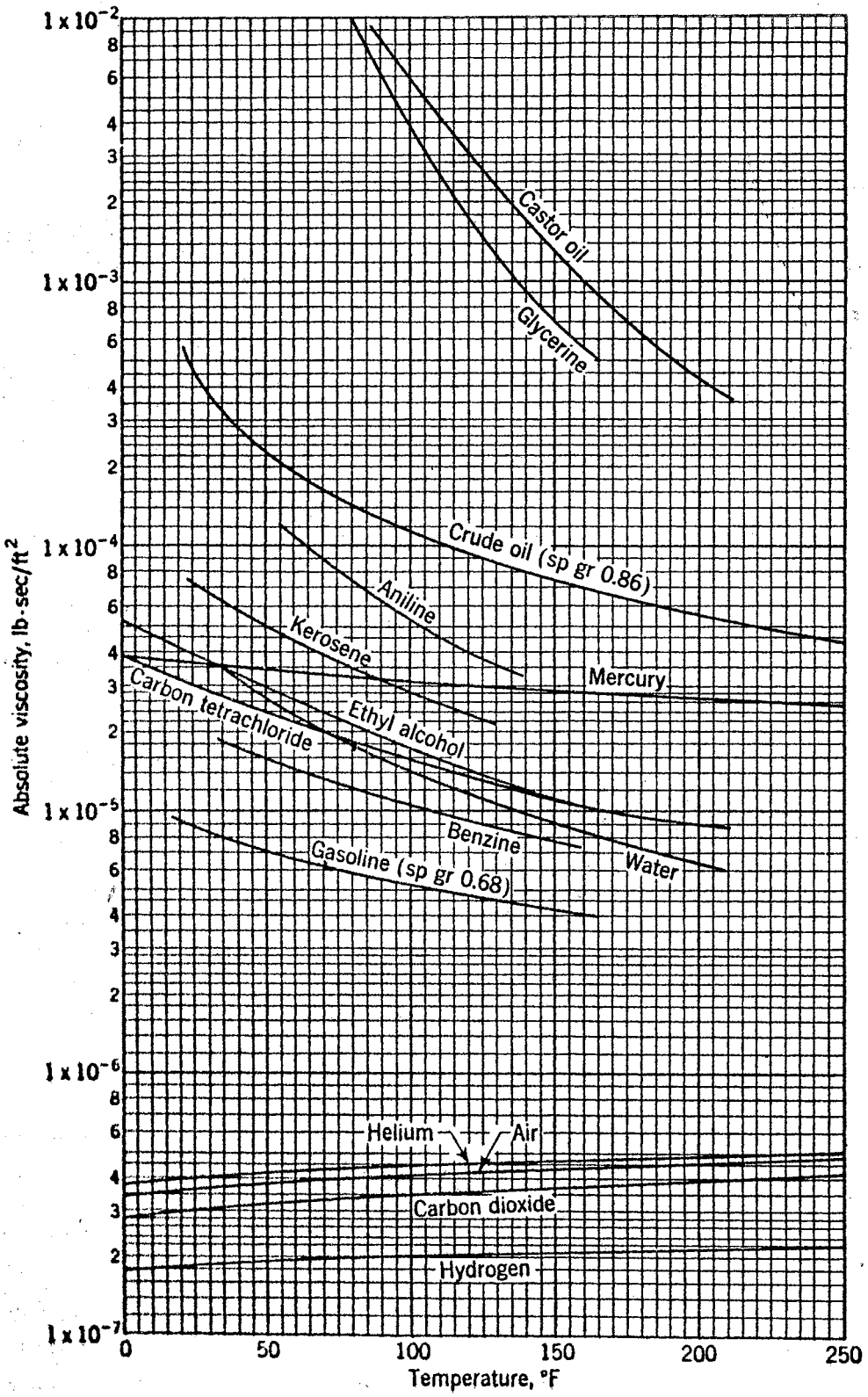

Figure 11. The Absolute Viscosities of Certain Gases and Liquids

VITA

Edward Fenton Cooke, III

Candidate for the Degree of

Master of Science

Thesis: THE PRECISION PRODUCTION OF UNIFORM DROPLETS

Major Field: Mechanical Engineering

Biographical:

Personal Data: Born in Beaumont, Texas, August 28, 1938, the son of Edward Fenton and Eva Cooke, Jr.

Education: Attended public school in Beaumont, Texas, graduating from Beaumont High School in 1956; completed requirements for the Bachelor of Arts degree from Rice University, with a major in Mechanical Engineering in June, 1960; received the Baker Foundation Scholarship in 1960 to aid in the completion of requirements for the Bachelor of Science degree in Mechanical Engineering; received the Bachelor of Arts degree and the Bachelor of Science degree, with a major in Mechanical Engineering, from Rice University in June, 1961; passed the Engineer in Training Examination in May, 1961; completed requirements for the Master of Science degree in August, 1962.

Professional Organizations and Experience: Member of American Society of Mechanical Engineers; member of Rice Engineering Society; Ensign in The United States Navy, June, 1961; employed by Gulf States Utilities in the project engineering division in the summer of 1957; employed by Gulf States Utilities in the relaying division in the summer of 1958; summer, 1960, redesigned, supervised, constructed electron beam furnace for Rice University; September, 1961 to May, 1962, instructor in engineering drawing course at Oklahoma State University; redesigned and supervised construction of water table for Oklahoma State University, summer, 1962.